Analysis of a Cylindrical Dielectric Radome Covering Omnidirectional Waveguide Slot Antennas

[1]J.-Y. Li, [2]J.-Li Guo, [2]Y.-L. Zou, and [2]Qi-Z. Liu

[1] Temasek Laboratories, National University of Singapore
Email: tsllijy@nus.edu.sg

[2] National Key Laboratory of Antennas and Microwave Technology, Xidian University

Abstract – In this paper, the method of moments (MoM) is employed to solve the electromagnetic field integral equation for characterizing slotted waveguide antenna covered by a dielectric radome. Different from those existing practical examples discussed in literature, these structures consist of mixed conducting and homogeneous dielectric objects. Both basis functions and testing functions are chosen as the well-established Rao-Wilton-Glisson (RWG) basis functions. Effects of the radome on the slotted antenna's radiation patterns are analyzed and discussed.

Keywords: Slot antenna, radiation pattern, method of moments, and radome.

I. INTRODUCTION

Omnidirectional waveguide slot array antennas are widely used in communication systems and beacon radar systems. This kind antenna arrays are easily designed and manufactured. They also have low profiles and high gains. The omnidirectional waveguide-slot array antennas have been used in practice for many years since the first experimental work [1]. Later, Lyon and Sangster [2] and Lü [3] theoretically analyzed waveguide slots and a slot-pair by employing the method of moments (MoM) to solve the resultant integral equations for the equivalence magnetic currents. An analysis of omnidirectional waveguide slot-pair in a standard rectangular (both air-filled and dielectric-filled) waveguide was carried out by Sangster and Wang [4]. Recently, Li [5] introduced a way to compute the radiation pattern of the omnidirectional waveguide slot-pair.

Usually, this type antenna must be covered by a radome in the communication system. Then, the radiation pattern of the slot antenna will degrade due to the effects of the radome. The RCS of dielectric material objects is analyzed by [6]. The scattering problems of mixture of conducting and dielectric objects are analyzed in [7-8]. Characterization of radiation by waveguide slot antenna with an arbitrarily shaped radome is an important subject for the communication systems, but it is also a difficult task. In this paper, radiation patterns of a slot-pair array covered by a radome are studied. The integral equation consisting of electric field integral equation and magnetic field integral equation is solved directly using the method of moment with Rao-Wilton-Glisson (RWG) basis functions [9].

The paper is organized as follows. In the next section, we will briefly present necessary mathematical formulations for the problem with mixed conducting and dielectric objects located in an isotropic free space medium at first. We outline how the method of moments is applied to solve the problem of waveguide slot antenna covered by a cylindrical radome. The RWG functions [9] are used as the basis and testing functions in the present the Galerkin's procedure. In the third section, numerical examples are presented so as to depict radiation patterns of several selected examples and the results of these examples are obtained and compared with available data.

II. DESCRIPTION OF FORMULATION

The equations defined here for electromagnetic scattering by mixed dielectric and electric conducting objects of arbitrary shapes are quite well established. As shown in Fig. 1, an example of an arbitrarily shaped homogeneous scatterer next to a conducting object is considered.

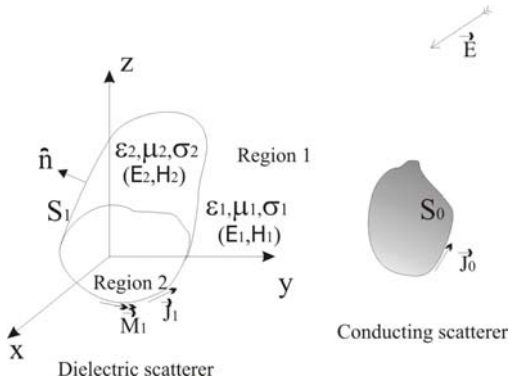

Fig. 1. Geometry of a dielectric scatterer and a conducting scatterer in an isotropic free space medium as a general configuration for the later radome analysis applications.

The permittivity and permeability of the dielectric scatterer are represented by ε_2 and μ_2, respectively. The scatterer is immersed in an infinite and homogeneous medium of permittivity ε_1, and permeability μ_1. In most applications, this infinite medium is free space.

Let $\vec{J}_1(\vec{r})$ and $\vec{M}_1(\vec{r})$ represent equivalent electric and magnetic currents on the surface of the homogeneous object. $\vec{J}_0(\vec{r})$ represents the equivalent electric surface current on the conducting object. Applying the equivalent principle to this electromagnetic problem, and considering the boundary condition, we obtain the electric and magnetic field integral equations below,

$$\vec{E}^1(\vec{r})|_{\tan} = \left\{ \left[j\omega\vec{A}_{11} + \nabla V_{11} \right] + \left[j\omega\vec{A}_{21} + \nabla V_{21} \right] + \left[\frac{1}{\varepsilon_1'} \nabla \times \vec{F}_{11} + \frac{1}{\varepsilon_2'} \nabla \times \vec{F}_{21} \right] + \left[j\omega\vec{A}_{10} + \nabla V_{10} \right] \right\} \Big|_{\tan} \quad (1a)$$

$$\vec{H}^1(\vec{r})|_{\tan} = \left\{ -\left[\frac{1}{\mu_1} \nabla \times \vec{A}_{11} + \frac{1}{\mu_2} \nabla \times \vec{A}_{21} \right] + \left[j\omega\vec{F}_{11} + \nabla U_{11} \right] + \left[j\omega\vec{F}_{21} + \nabla U_{21} \right] - \frac{1}{\mu_1} \nabla \times \vec{A}_{10} \right\} \Big|_{\tan} \quad (1b)$$

for $\vec{r}$ on the surface S_1;

$$\vec{E}^0(\vec{r})|_{\tan} = \left\{ \left[j\omega\vec{A}_{11} + \nabla V_{11} \right] + \left[\frac{1}{\varepsilon_1'} \nabla \times \vec{F}_{11} \right] + \left[j\omega\vec{A}_{10} + \nabla V_{10} \right] \right\} \Big|_{\tan} \quad (1c)$$

for $\vec{r}$ on the surface S_0,

where $\vec{E}^1(\vec{r})$, $\vec{H}^1(\vec{r})$ and $\vec{E}^0(\vec{r})$ stand for the incident electric and magnetic fields in region 1 and the subscript "tan" refer to tangential components on the surfaces, S_1 and S_0. The vector potentials, $\vec{A}_{i1}(\vec{r})$ and $\vec{F}_{i1}(\vec{r})$ for $i = 1,2$, and the scalar potentials, $V_{i1}(\vec{r})$ and $U_{i1}(\vec{r})$, are given by,

$$\vec{A}_{i1} = \vec{A}_{i1}(\vec{r}) = \frac{\mu_i}{4\pi} \int_S G_i(\vec{r},\vec{r}') \cdot \vec{J}_1(\vec{r}') dS' \quad (2a)$$

$$\vec{F}_{i1} = \vec{F}_{i1}(\vec{r}) = \frac{\varepsilon_i'}{4\pi} \int_S G_i(\vec{r},\vec{r}') \cdot \vec{M}_1(\vec{r}') dS' , \quad (2b)$$

$$V_{i1} = V_{i1}(\vec{r}) = \frac{1}{4\pi\varepsilon_i'} \int_S G_i(\vec{r},\vec{r}') \cdot \rho_1^e(\vec{r}) dS' , \quad (2c)$$

$$U_{i1} = U_{i1}(\vec{r}) = \frac{1}{4\pi\mu_i} \int_S G_i(\vec{r},\vec{r}') \cdot \rho_1^m(\vec{r}) dS' , \quad (2d)$$

$$\varepsilon_i' = \varepsilon_i - j\sigma_i/\omega , \quad (2e)$$

$$\rho_1^e(\vec{r}) = \frac{-1}{j\omega} \left[\nabla' \cdot \vec{J}_1(\vec{r}') \right] , \quad (2f)$$

$$\rho_1^m(\vec{r}) = \frac{-1}{j\omega} \left[\nabla' \cdot \vec{M}_1(\vec{r}') \right] , \quad (2g)$$

$$\vec{A}_{10} = \vec{A}_{10}(\vec{r}) = \frac{\mu_i}{4\pi} \int_S G_1(\vec{r},\vec{r}') \cdot \vec{J}_0(\vec{r}') dS' , \quad (2h)$$

$$V_{10} = V_{10}(\vec{r}) = \frac{1}{4\pi\varepsilon_i'} \int_S G_1(\vec{r},\vec{r}') \cdot \rho_0^e(\vec{r}) dS' , \quad (2i)$$

$$\rho_0^e(\vec{r}) = \frac{-1}{j\omega} \left[\nabla' \cdot \vec{J}_0(\vec{r}') \right] . \quad (2j)$$

The Green's functions, $G_i(\vec{r},\vec{r}')$ where $i = 1,2$, have the following form,

$$G_i(\vec{r},\vec{r}') = \frac{e^{-jk_iR}}{R} \quad (3)$$

where $R = |\vec{r} - \vec{r}'|$ and,

$$k_i = \omega\sqrt{\mu_i\varepsilon_i'} \quad . \quad (4)$$

Equations (1a-1c) are solved by applying the method of moments. In this work, all the surfaces of scatterers are approximated by planar triangular patches and thus the RWG functions [9] are chosen as both basis functions and testing functions. As in a conventional MoM solution, the unknown surface electric and magnetic current distributions $\vec{J}_1(\vec{r})$, $\vec{M}_1(\vec{r})$, and $\vec{J}_0(\vec{r})$ are expanded into three sets of basis functions $\{\vec{f}_n^1(\vec{r})\}$, $\{\vec{f}_n^1(\vec{r})\}$ and $\{\vec{f}_n^0(\vec{r})\}$ as follows,

$$\vec{J}_1(\vec{r}) = \sum_{n=1}^{N_d} I_n^1 \cdot \vec{f}_n^1(\vec{r}) \tag{5a}$$

$$\vec{M}_1(\vec{r}) = \sum_{n=1}^{N_d} M_n^1 \cdot \vec{f}_n^1(\vec{r}), \tag{5b}$$

$$\vec{J}_0(\vec{r}) = \sum_{n=1}^{N_c} I_n^0 \cdot \vec{f}_n^0(\vec{r}) \tag{5c}$$

where N_d and N_c stand for the numbers of edges on the dielectric and conducting surfaces of the triangular model, respectively. After applying the method of moments to equations (1a-1c), the equations are converted into a system of N linear equations and are further written in matrix form as follows,

$$\begin{bmatrix} Z_{11} & Z_{12} & Z_{13} \\ Z_{21} & Z_{22} & Z_{23} \\ Z_{31} & Z_{32} & Z_{33} \end{bmatrix} \cdot \begin{bmatrix} I_1 \\ M_1 \\ I_0 \end{bmatrix} = \begin{bmatrix} E_1 \\ H_1 \\ E_0 \end{bmatrix} \tag{6}$$

where the impedance matrix is of dimension NxN with N = N_d + N_c, and all the elements in equation (6) are sub-matrixes [8].

For a scattering problem, the right-hand side of equation (6) may be written,

$$E_{1j} = \int_{S_1} \vec{f}_j^1(\vec{r}) \cdot \vec{E}^1(\vec{r}) dS \tag{7}$$

$$H_{1j} = \int_{S_1} \vec{f}_j^1(\vec{r}) \cdot \vec{H}^1(\vec{r}) dS\ , \tag{8}$$

$$E_{0j} = \int_{S_1} \vec{f}_j^0(\vec{r}) \cdot \vec{E}^0(\vec{r}) dS\ . \tag{9}$$

For the radiation problem, one can set a voltage source in the excitation port. However, only a few elements of E^0 in equation (6) are assigned to be nonzero values.

For the geometry of slotted waveguide antennas covered by a cylinder radome in this paper, a short dipole is placed in the waveguide as the exciting source when we analyze the radiation characteristics of the slotted-waveguide antennas.

III. NUMERICAL RESULTS

Based on the theoretical formulas and MoM, a code is written in fortran language for simulating the waveguide slot array with radome and scattering from hybrid metallic-dielectric objects. To examine the correctness of the code, we first investigate bistatic radar cross sections (RCSs) of a conducting sphere next to an air-filled dielectric sphere. The RCS results are obtained for a plane wave of $\theta\theta$-polarization, with an incidence angle of $\theta = 0^o$ and $\varphi = 90^o$. The results are shown in Fig. 2 where the "Conducting sphere only" results were obtained using the EFIE in the absence of the dielectric objects. Two cases are considered here, one (with 1,200 unknowns) for a conducting sphere of 1 meter radius only, and the other (with 3,600 unknowns) for a conducting sphere of 1 meter radius next to a dielectric sphere of 1-meter radius (which is also considered as a special case, we considered $\varepsilon_r = 1$, $\mu_r = 1$, and $\sigma = 0$, and the distance is 3 meters in the y-direction). A good agreement between the numerical results for both cases is observed in Fig. 2; and certainly the agreement is expected. This indicates that the results produced by the code are reducible to those of special cases, partially verifying the correctness of the code.

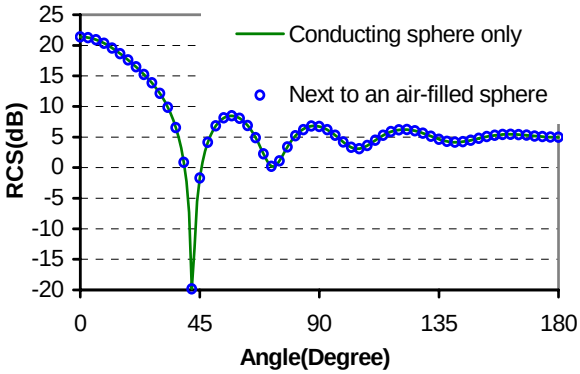

Fig. 2. Bistatic RCS of a sphere at $f = 0.3$ GHz.

The geometer of radome and slotted waveguide are shown in Figs. 3 (a) and (b). The axis of cylinder radome is along z direction. The slotted waveguide is put in the center of the radome along the axis. The radome is open in the bottom and is closed on the top. The height of cylinder radome is 90mm. The radii (R), the depth (D) and the permittivity (ε_r) of the radome are chosen with different values for analyzing the effect of the radome. The slotted waveguide with radome is analyzed as following.

The selected working frequency is 9.375 GHz here. The width of the waveguide is 22.86 mm. The height of waveguide is 1 mm. The total length of waveguide is 1.3 λ_g. The depth of waveguide is 1 mm. One end of the waveguide is shorted, and the dipole is placed near another end (0.25 λ_g, λ_g = 44.8036 mm). The width of the slots is 1.00 mm. Two slot-pairs are cut on the waveguide walls. The distance between the two slot-pairs is 0.5 λ_g.. The length of the slot is 13.90 mm, the offset of the slot-pair is 1.00 mm, the slot center located at 0.25 λ_g away from the shorted plug.

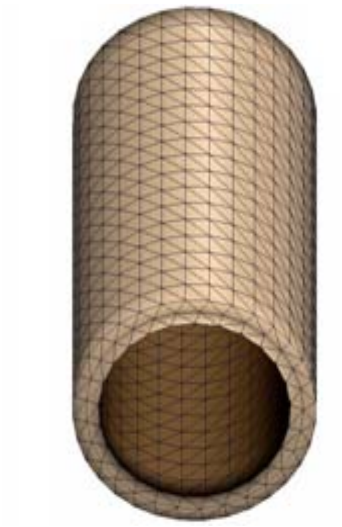

(a) Radome.

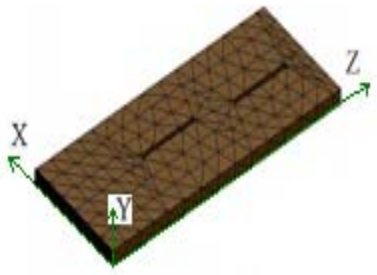

(b) slotted waveguide.

Fig. 3. Radome and slotted waveguide antenna.

To further verify the correctness and capability of our code and the idea for analyzing the slotted waveguide, the radiation patterns of the waveguide slot antenna (with air-filled radome, set ε_2=1.0) are computed first. The results are presented in Fig. 4 where both the *E*- and *H*-plane patterns are shown. The *E*-plane and *H*-plane patterns are in x-y plane (θ=90°, ϕ turns from 0° to 360°) and y-z plane (ϕ=90°, θ turns from 0° to 360°), respectively. All the radiation patterns are normalized.

A good agreement between the numerical results of both the air-filled radome case and no radome case is observed. This indicates that the results produced by the code are reducible to those of special cases, partially verifying the correctness of the code and the analysis way.

Different parameters of the radome, namely, the radii (*R*), the depth (*D*) and the permittivity (ε_r), are chosen subsequently for analyzing the effects of the radome. The radii (*R*) are chosen to be: (1) 0.5λ; (2) 0.6λ; (3) 0.65λ; and (4) 0.75λ. The depths (*D*/λ) are assumed to be (1) 0.125; (2) 0.1764; (3) 0.25. The relative permittivities of ε_2 are chosen as (1) 2; (2) 3; and (3) 4.

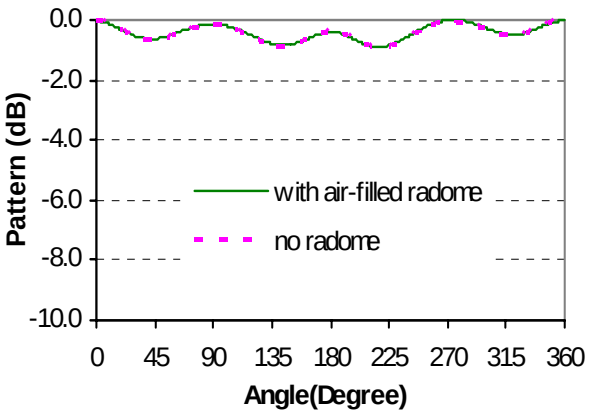

(a) *E*-plane (θ=90°, ϕ changes from 0° to 360°).

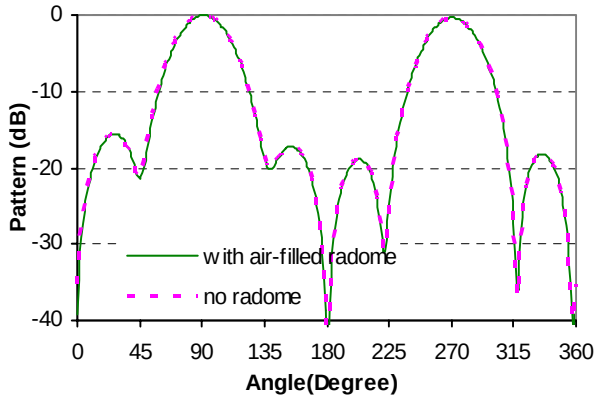

(b) *H*-plane (ϕ=90°, θ changes from 0° to 360°).

Fig. 4. The computed far field patterns of slot-pair.

First of all, we consider the variation of the relative permittivity of the dielectric radome and the radome's radius. The computed results are presented in Figs. 5-7 where the radii (*R*) and the permittivities (ε_r) of the radome are different, and the depth is chosen as 0.125λ. When the radius (*R*) are half a wavelength (*i.e.*, 0.5λ), the *E*-plane and *H*-plane far-zone patterns are both poor. It is however realized that if the radii (*R*) are chosen as 0.6λ and 0.65λ, respectively, the roundness of *E*-plane pattern is better when different permittivities (ε_r) are used. The effects due to permittivity changes are apparently very significant. If ε_r = 2, effects of radii (*R*) becomes less important, but if ε_r increases to be higher in value, we must be very careful to choose appropriate radii of the radome to maintain the generally overall good performance of the antenna. Therefore, it is very important for a radome designer to know clearly what kind of effects will be caused by changing the configurations of the whole system during the antenna and its dielectric radome designs.

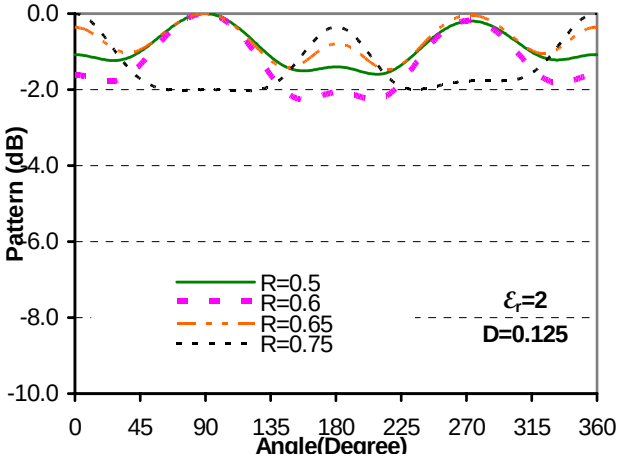

(a) *E*-plane.

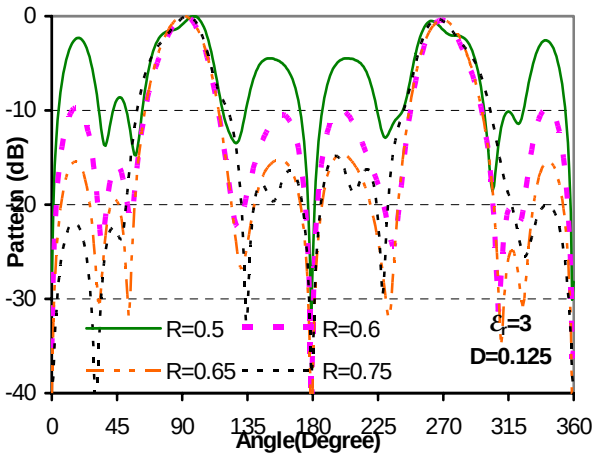

(b) *H*-plane.

Fig. 6. The computed far field patterns of the slot-pair.

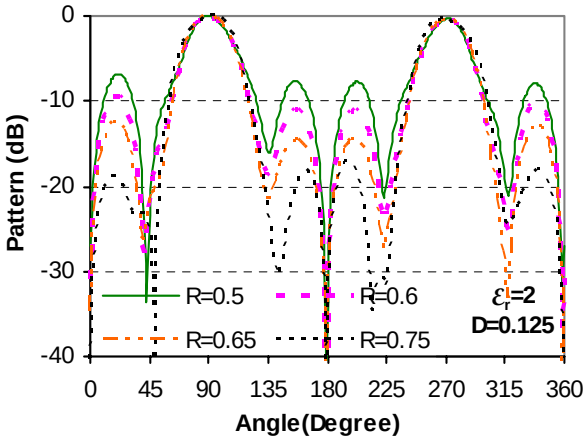

(b) *H*-plane.

Fig. 5. The computed far field patterns of the slot-pair.

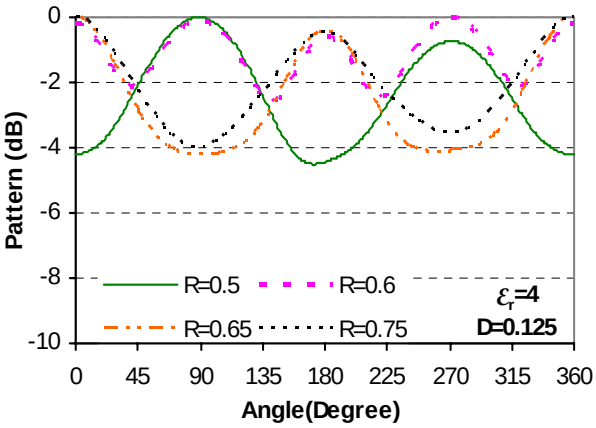

(a) *E*-plane.

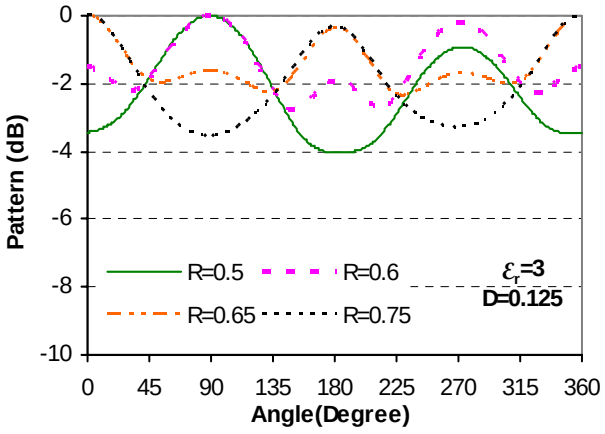

(a) *E*-plane.

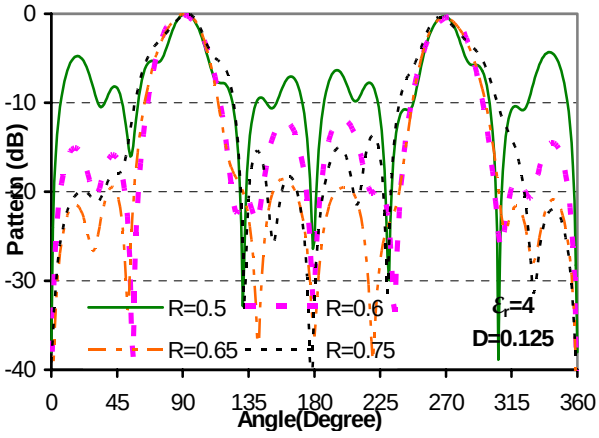

(b) *H*-plane.

Fig. 7. The computed far field patterns of the slot-pair.

Subsequently, computed results (when the depth is chosen as 0.1764λ) are presented in Figs. 8-10 where the radii (R) and the permittivities (ε_r) of the radome vary. When the radii (R) are chosen to be 0.5λ and 0.75λ, respectively, the E-plane and H-plane antenna patterns are both poor. If the radii (R) are chosen as 0.6λ and 0.65λ, respectively, the E-plane pattern is apparently improved when the different permittivity (ε_r) values are used.

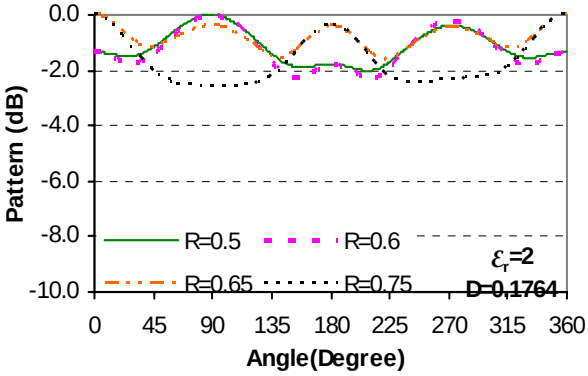

(a) E-plane.

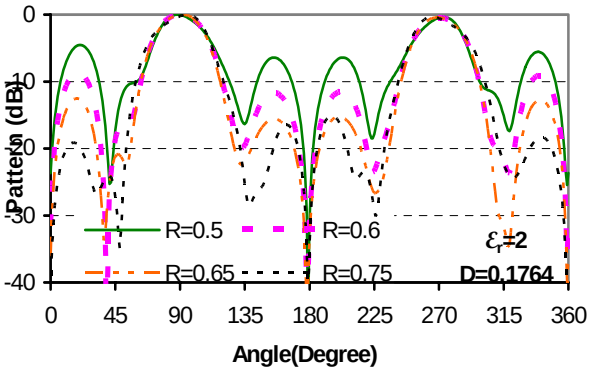

(b) H-plane.

Fig. 8. The computed far field patterns of the slot-pair.

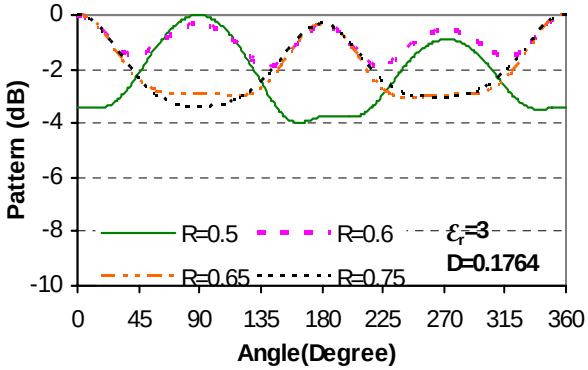

(a) E-plane)

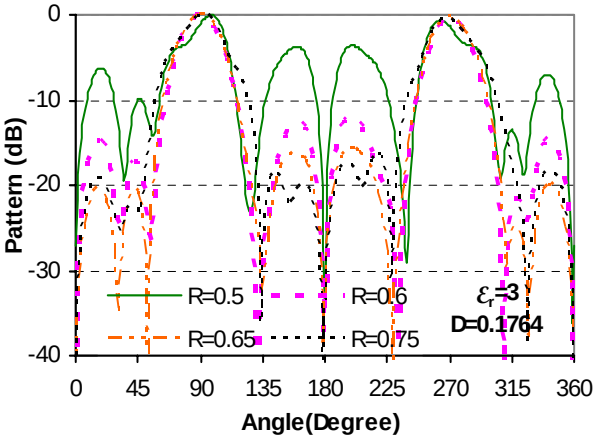

(b) H-plane

Fig. 9. The computed far field patterns of the slot-pair.

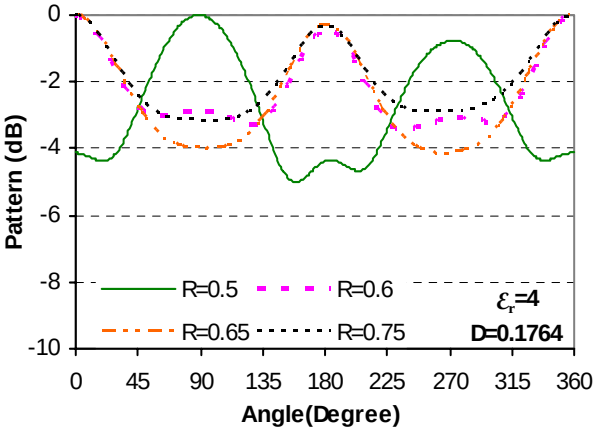

(a) E-plane

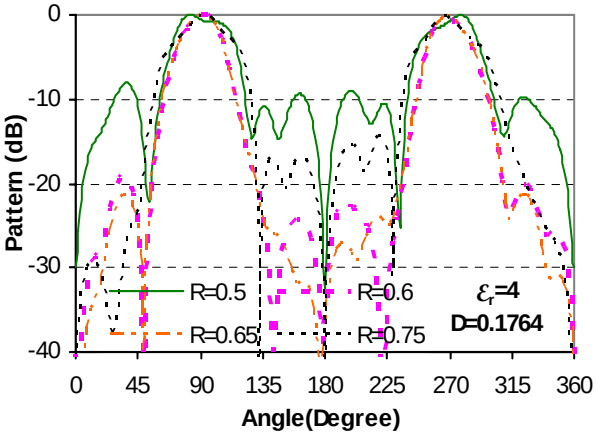

(b) H-plane.

Fig. 10. The computed far field patterns of the slot-pair.

Finally, the radiation patterns are obtained for a depth of 0.25 λ and different radii (R) and permittivity (ε_r) values. The obtained results are shown in Fig. 11. The E-plane and H-plane patterns are found both very good and the distortion due to the radome is very minimal. It is shown that when the radome is designed, the radii (R) of the cylindrical radome are preferably chosen as 0.6λ and 0.65λ so as to provide desired antenna patterns.

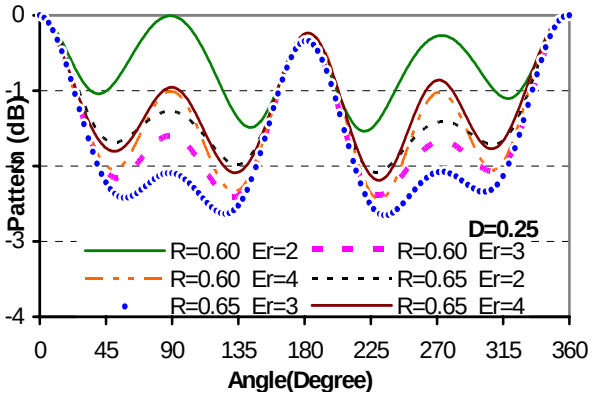

(a) E-plane.

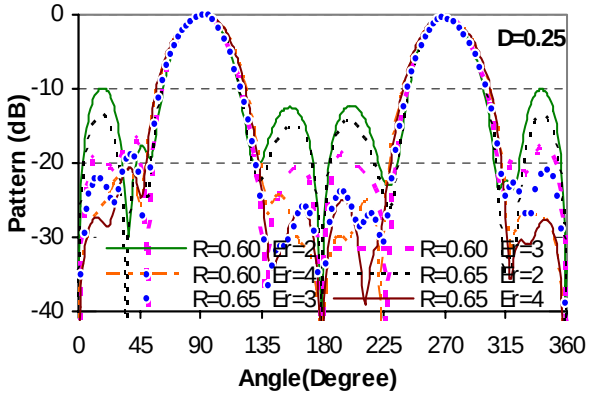

(b) H-plane.

Fig. 11. The computed far field patterns of the slot-pair where Er denotes permittivity.

IV. CONCLUSION

In this paper, the method of moments is employed to analyze waveguide slot antenna in the presence of a dielectric radome. The detailed electromagnetic field integral equation formulations for radiation (and scattering) by these antennas (and scatterer) of arbitrarily shaped 3D geometry are carried out. The Galerkin's MoM procedure is utilized to solve the integrate equations. Some numerical examples are considered and their results are shown to verify the correctness of formulations and capability of our numerical codes. The waveguide slot antennas with radome (as the examples) are analyzed in detail.

REFERENCES

[1] T. Takeshima, "X-band omnidirecrectional double-slot array antenna," *Electron Eng.*, vol. 39, pp. 617–621, Oct. 1967.

[2] S. W. LÜ, "Study of properties of slot-pair in waveguide," *ACTA Electronica Sinica*, vol. 16, pp. 104–107, Sept. 1988. (in Chinese)

[3] R. W. Lyon and A. J. Sangster, "Efficient moment method analysis of radiating slots in a thick-walled rectangular waveguide," *Proc. Inst. Elect. Eng. Part H*, vol. 128, pp. 197–205, Aug. 1981.

[4] A. J. Sangster and H. Wang, "Resonance properties of omnidirectional slot doublet in rectangular waveguide," *Electronics Letters*, vol. 29, no. 1, pp. 16–18, 1993.

[5] J. Y. Li, L. W. Li, and Y. B. Gan, "Method of moments analysis of waveguide slot antennas using the EFIE," *Journal of Electromagnetic Waves and Applications*, vol. 19, no. 13, pp. 1729-1748, 2005.

[6] K. Umashankar, A. Taflove, and S. M. Rao, "Electromagnetic scattering by arbitrary shaped three-dimensional homogeneous lossy dielectric objcts," *IEEE Trans. on Antennas and Propagation,* vol. 34, no. 6, pp. 758–766, June 1986.

[7] B. M. Kolundzija, "Electromagnetic modeling of composite metallic and dielectric structures," *IEEE Trans. on microwave theory and techniques,* vol. 47, no. 7, pp. 1021–1032, July 1999.

[8] J. Y. Li and L. W. Li, "Electromagnetic scattering by a mixture of conducting and dielectric objects: analysis using method of moments," *IEEE Trans. on Vehicular Technology,* vol. 53, no. 2, pp. 514–520, 2004.

[9] S. M. Rao, D. R. Wilton, and A. W. Glisson, "Electromagnetic scattering by surfaces of arbitrary shape, " *IEEE Trans. on Antennas and Propagation,* vol. 30, no. 5, pp. 409–418, May 1982.

Jian-Ying Li received the degrees of B.Sc. in Mathematics, and M.Eng.Sc. and Ph.D. both in Electromagnetic Field and Microwave Technology from Henan Normal University, Xinxiang, China, in 1986, and Xidian University, Xi'an, China, in 1992 and 1999, respectively. From 1992 to 1996, he worked at Xi'an Electronic Engineering Research Institute, Xi'an, China as a Research&Design Engineer. From 1999 to 2001, he was with the Department of Electrical and Computer Engineering at the National University of Singapore (NUS) where he was a Postdoctoral Research Fellow. From 2001 to 2003, he was with High Performance Computation for Engineered Systems (HPCES)

Programme at the Singapore-MIT Alliance (SMA), as a Research Fellow. Currently, he is a Research Scientist of Temasek Laboratories, National University of Singapore. His main research interests include fast algorithms in computational electromagnetics, wave propagation and scattering, design and analysis of phased arrays, waveguide slot antennas, and microstrip antennas, and broadband electrical small antennas etc.

Jing-Li Guo received the B.Eng. and M.Eng., and Ph.D degrees all in Electronic Engineering from Xidian University, Xi'an, China, China in 1999, 2002 and 2005, respectively.

Currently, she is a Lecturer in the National Key Laboratory of Antennas and Microwave Technology, Xidian University. Her research interests include antenna array, broadband miniature antenna analysis and design, computation electromagnetic, and EMC.

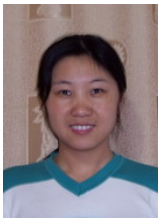

Yan-Lin Zou received the B.Eng. and M.Eng. degrees in electronic engineering from Xidian University, Xi'an, China, in 2002 and 2005, respectively. Currently, she is a Doctor candidate and a Lecturer in the National Key Laboratory of Antennas and Microwave Technology, Xidian University. Her research interests include smart antenna, broadband electrically small antenna, antenna array, computation electromagnetic.

Qi-Zhong Liu was born in Sichuan, China, in 1938. He is now a professor of the National Key Laboratory of Antennas and Microwave Technology, Xidian University. He is the editorial member of Chinese Journal of Radio Science and the senior member of Chinese Institute of Electronics. His research interests include analysis and design of array antenna, smart antenna, broadband miniature antenna, computation of RCS, and EMC.